Assimilation of lidar planetary boundary layer height observations

Andrew Tangborn, Belay Demoz, Brian Carroll, Joseph Santanello and Jeffrey Anderson

Response to reviewer 2

I'd like to thank the authors for answering my questions and addressing my concerns. The manuscript overall is better.

Regarding my previous PBLH definition question, I understand that the authors would like to defer the evaluation/discussion to future work. Having said that, as it is important to understand the nature of the observation operator and use corresponding model variable for data assimilation, I would suggest the authors to add in the conclusions saying that the observation operator and the model variable "issue" still needs to be addressed.

We have added a sentence to this effect.

Minor comments:

Line 324: the sentence "particulary when this approach is applied to an EnKF assimilation system with cycling" should be removed. If I understand correctly, the experiments performed in this work are stand-alone analysis, no forecasts are issued from the analyses, and no cycling is involved.

This sentence is actually in line 291. And it was meant to describe a hypothetical EnKF. We have added some additional wording to indicate that this is for future efforts to build a cycling EnKF.

Figure numbers are shown as ?? in the manuscript.

This is occurs in the version of the paper that shows the changes from the previous manuscript, and since they have a different number of figures, some (or perhaps all) appear as ??. You should be able to see the correct figure numbers in the revised manuscript.

Response to reviewer 4

Major comments

1. The presentation of the data assimilation results needs to be refined.

(a) Interpretation of the observation misfits On L245-L248, the authors justify the small analysis increments in the early morning hours by noting the small deviation between the forecasted thermodynamic and kinematic profiles from the corresponding radiosonde measurements. This conclusion in not consistent with the EnOI update because the innovation $d = y - h(x)$ only refers to the misfit between observed and forecasted (diagnosed) PBLH values. L248-L249 correctly state that there are relatively large misfits between the observed and prior PBLH, but the authors do not emphasize that these differences control the subsequent corrections of the prior T, MV, U and V profiles.

You are correct in that the profiles do not directly impact the analysis increments since PBLH is the only observed quantity assimilated here. And it is also true that the state variables at a given time will impact the PBLH at a later time, and therefore the correction then as well. We have revised these sentences to make it clearer.

(b) The role of prior ensemble spread in the model space corrections I also think that the authors need to better quantify the origin of the analysis increments in model space. From Eqs. (2) and (3), it should be clear that the magnitude of the model state corrections depends on two distinct factors: (i) the ensemble cross-covariances $P^f H^T$ and (ii) the scaled innovation $d = R + HPfH^T/(y - h(x^f))$. To justify the observed differences between the model state corrections in the early morning and late afternoon hours, the authors focus on the magnitude of the ensemble covariances (Fig. 8), but pay little attention to how the background ensemble spread in observation space ($HP^f H^T$) affects the scaled PBLH misfit d . Aside from contributing to a more complete understanding of the model state corrections, examination of the prior PBLH spread will also shed some light on the underlying forecast uncertainty.

We agree that this is an important comparison to make. We have added a figure that shows both HP^fH^T and R at the 6 times when the sonde data is available, and these indicate that R is much larger during the times when there is little impact from the assimilation.

(c) Discussion of the PBLH corrections While I agree with the authors' approach of focusing on the model state increments, a brief discussion of the PBLH corrections is also warranted. Such a discussion is important because the PBLH increments have a direct impact on the subsequent model state corrections (e.g., Anderson 2003). Intuitively, if a data assimilation system is not effective in estimating the directly observed quantities, it will also struggle to constrain the unobserved model state variables. Therefore, I encourage the authors to elaborate on the extent to which the analyzed PBLH values were able to move closer to the independent radiosonde-based PBLH retrievals.

We are assuming that you are not asking if the analysis estimate of PBLH is closer to the observations than the forecast estimate. This would be trivially true, and not important because the analysis PBLH is not a prognostic variable and will have no impact on the next forecast. Instead, we think you mean that are the temperature and moisture analysis fields likely to produce a better PBLH if they were passed through the PBL physics package (which is not done in this work). We can say with some confidence that we think it would improve the PBLH. For example, the height potential temperature profiles can be seen to rise is much closer to the observed PBLH for the analysis. This indicates that the PBL scheme would likely produce a more accurate PBLH from the analysis, and possibly for the next forecast. We have added some comments in the text to explain this.

2. I found the authors' justification on the importance of assimilating PBLH retrievals particularly appealing (L102-L104), but the literature overview on past efforts of assimilating Doppler lidar measurements (L99-L104) needs to be corrected and expanded. First, none of the cited studies (Hu et al. 2019; Coniglio et al. 2019; Degelia et al. 2019) report improvements to the PBLH; instead they examine the forecast performance with respect to convective initiation. Second, the aforementioned papers assimilate horizontal wind profiles derived from the VAD technique. This comes in contrast with other studies (e.g., Kamineni et al. 2003) which focus on the impacts from assimilating thermodynamic lidar profiles. To put this study into a broader context, I suggest that the authors place more emphasis on the aforementioned differences and further expand on their literature overview starting on L98. Apart from discussing the past efforts referenced above, the authors should also include some of the most recently published research in this area. For instance, both Degelia et al. (2020) and Chipilski et al. (2020) assimilate Doppler lidar retrievals in the context of nocturnal convective systems. Chipilski et al. (2020) additionally reveal that the assimilation of Doppler lidar wind data affects the characteristics of the stable PBL – a finding which is particularly relevant in the context of the present study.

We have revised the discussion on assimilation of profile observations, including discussion of the Chipilski (2020) abnd Degelia (2020) papers. And we have connected these to works to this paper by adding a couple of sentences on convective initiation withn the PBL.

3. A critical discussion is also needed to highlight the future challenges of assimilating PBLH retrievals. The authors point out that their work is a "necessary first step in terms of how ensemble statistics can help to constrain profiles within the PBL", indicate the need to assimilate PBLH retrievals in real-time EnKF systems under diverse weather regimes, but provide little information on the specific problems of assimilating the PBLH variable. Given that this paper is designed to inform the future incorporation of PBLH retrievals into real-time data assimilation systems, the authors should elaborate on what the most outstanding challenges in this area are. The bullet points below provide a couple of suggestions: while I certainly do not expect the authors to follow all of them, I encourage their incorporation with some of the authors' own concerns.

· The calculation of PBLH is different in model simulations and observations: while the observed PBLH is derived from Doppler lidar measurements of turbulence intensity, horizontal wind profiles and backscatter intensity, the prior PBLH is diagnosed using the specific formulation of a particular PBL scheme. Each of these two methods has its own approximations and, perhaps even more importantly, will not yield the same PBLH value even if the simulated and observed meteorological conditions are identical. If such biases are not taken into account, the analysis estimate produced by Eq. (3) will be suboptimal. The aforementioned methodological differences also constitute a problem from the viewpoint of forecast verification.

We have added a couple of sentences on the need to study a wide variety of PBL physics schemes with

this assimilation approach. While the different methods to compute PBLH from radiosonde data add to the uncertainty, it's not as important here because we are not trying to improve estimates of the PBLH, but rather improve the state variable forecast within the PBL.

· *Treatment of observations errors. On L166, it is stated that the observation error variances are equal to the uncertainty estimates provided by the lidar retrievals. In additional to these measurement errors, operational data assimilation systems typically also consider (i) errors of representation and (ii) errors due to approximations in the observation (forward) operator. These additional error contributions might be important to consider in future efforts. For example, errors of representativity might be especially relevant within the more inhomogeneous stable PBL, whereas the methodological differences in the PBLH computation could be treated, at least to a first degree, as errors in the observation operator.*

This is an important issue, and it relates to the different physics schemes since they implicitly represent the forward operator. This is why it is important to conduct assimilation experiments with a number of different schemes, and the resulting impact on the state variable profiles should give a good indication as to whether the ensemble generated forward operator is accurately representing correlations. Some increase in the observation error shoiuld be included here as well. We have added a sentence on this in the Discussion and conclusions section.

· *The ability of PBLH retrievals to efficiently constrain the model state. Here I offer two different comments. The first one concerns the inability of PBLH retrievals to correct the stable PBL structure despite the large differences in the prior and observed PBLH values. The analysis offered by the authors indicates that the lack of ensemble cross-covariances is a likely explanation. This raises the question, however, whether the small corrections in stable PBLs constitutes a systematic effect induced by the formulation of current PBL schemes. Answering this question is important as one of the focal objectives of the PECAN field campaign was to understand if the information provided by ground-based PBL profilers can improve the traditionally poor forecasts of nocturnal convective systems. The second point the authors might want to consider is how effective the PBLH retrievals would be in the context of other observation networks. A past NRC report (NRC 2009) describes the potential deployment of a nation-wide network of thermodynamic and kinematic PBL profilers, quite similar to the ones employed during the PECAN field campaign. Unlike the ceilometer network that originally motivated this study, the PBL profilers will produce direct observations of model state variables that could make the ceilometer-based PBLH retrievals redundant.*

We agree with these concerns. The new plot showing the relative values for $\mathbf{R}$ and $\mathbf{HP}^f\mathbf{H}^T$ over time indicate that the uncertainty in the lidar observations during the night is a big part of the reason. So it would be very helpful to have profile (thermodynamic and kinetic) profiles during this time to complement the PBLH observations. We have added this to the Summary and Conclusions section.

· *My last comment is more technical in nature and relates to the theoretical inappropriateness of current data assimilation systems to extract information from PBLH retrievals. By definition, PBLH is a non-negative quantity. As such, it faces the problems similar to those associated with the assimilation of certain moisture variables (e.g., specific humidity; see Dee and da Silva 2003). Because PBLH is a bounded quantity, its distribution will not always be Gaussian. Hence, traditional assumptions used to derive operational data assimilation schemes will be violated (e.g., Bocquet et al. 2010; Bannister et al. 2020). Such deviations from Gaussianity will be particularly visible under stable PBLs (because PBLH is closer to its lower bound of 0m), further complicating the data assimilation problems already noted in this manuscript. It might be possible to remedy the problem of boundedness by adopting certain non-Gaussian extensions of traditional data assimilation algorithms (cf. Cohn 1997; Fletcher and Zupanski 2006; Bishop 2016).*

PBLH assimilation may benefit from some of the above methods to deal with non-Gaussian statistics. WE have added a sentence to explain this.

Minor comments

1. *L32: Momentum is also exchanged in land-atmosphere interactions, please add to the list.*

done

2. L46-L47: "... since aerosols are well mixed throughout the PBL (Hicks et al., 2019)" - this statement is only valid in the context of CBL.

Statement has been changed to address this.

3. L72-L73: "... were not yet available for the campaign we are using". Before providing details on how the Doppler lidar measurements in Greensburg were obtained, the readers would benefit from a short description of the PECAN field campaign as a whole.

We have added several sentences to the introduction on the PECAN campaign.

4. The use of "PBLH retrievals" is more appropriate than "PBLH measurements" as it emphasizes that PBLH is a derived quantity. There are a couple of instances in the manuscript where this correction needs to be applied.

We have changed this wherever it occurs.

5. Description of the methods to assimilate the PBLH retrievals (L107-L109). It might be better to replace the statement "either by creating an adjoint of the PBL parameterization scheme" with "either by adopting a variational data assimilation scheme" (or a semantically equivalent expression). Formulating the adjoint of a parameterisation scheme is a specific implementation aspect of variational data assimilation algorithms. If the authors desire so, they could motivate their preference for an EnKF approach in this study by pointing out that ensemble-based methods sidestep the generally difficult task of linearizing the model physics equations.

We have made this change.

6. Please cite the original EnKF paper of Evensen (1994) and its subsequent refinement in Burgers et al. (1998) on L123.

done.

7. L124: "... where the analysis state is the estimate with the minimum estimated errors". The original derivation of the Kalman filter minimizes the expected squared errors. Note that the latter corresponds to a minimisation of an error norm rather than the error norm implied on L124.

We have changed the wording here.

8. The EnOI was originally introduced by Oke et al. (2002) and also discussed by Evensen (2003), so please make sure to add these references on L133.

Done.

9. On L141, the authors mention the names of the two parameterization schemes used in the archived NU-WRF simulations. A brief justification on why these two parameterization schemes were chosen in the original PECAN runs will be helpful.

These simulations were done on a previous project concerned with precipitation that I was involved with. They were chosen because the PBL scheme was the same for both, while the precipitation algorithm is different. It would have been more interesting for this project if we had a different PBL scheme to compare with, but it was not possible. I don't think this information would add any incite to the present work.

10. The abbreviation TKE on L145 is commonly used to denote "turbulent kinetic energy" in boundary layer research, so it might be best to consider rewording.

Done

11. State vector definition (L145-L148). Please clarify whether the state variable Q refers to specific humidity, mixing ratio or another moisture variable. The authors should also stress that the state vector $\mathbf{x}$ *in this study represents a vertical column, which is why* P^f *only refers to the vertical ensemble covariances.*

Done.

12. Mathematical description of the EnOI algorithm (L160-L191). Here I have a couple of technical remarks aimed at refining the mathematical presentation of the EnOI algorithm.

· Because the definition of the forecasted error covariance in Eq. (1) is too general and not specific to the EnOI algorithm, it might be best to remove it from the discussion.

We agree, since this form is never used in the algorithm. It has been removed.

· Similarly, it is not necessary to write the measurement equation $y - Hx$*; instead, the authors could simply state that* y *in Eq. (2) represents the PBLH observations retrieved from the Doppler lidar. (As a side comment, the aforementioned measurement equation is only partially complete in the context of filtering theory as it should include a random noise term.)*

We have made this change.

· It will be best to avoid mixing the vectorial and scalar notations in Eqs. (2) and (3). This could be done by first writing the general form of Eqs. (2)-(3) and then describing how these were solved by the EnOI algorithm employed in this study. Regarding the latter, the authors should highlight that y

as well as the corresponding HP^fH and R matrices are scalar quantities and that both PfH^T and HP^fH^T are computed from an ensemble of model profiles, as indicated by Eqs. (4) and (5).

We have rewritten these equations in the manner you suggested.

· A brief description is needed to explain how the vertical localization mentioned on L177- L185 was implemented in this study.

The vertical covariance is multiplied by the localization factor. We have added this detail.

13. Opening sentences in Section 3 (L193-L199). Some aspects regarding the description of the NU-WRF simulations were already discussed in the paragraph starting on L141. The missing details found on L193-L199 should be moved back to this paragraph.

This has been moved.

14. L205: "... in the late evening to early morning (2-7 UTC)". 7 UTC does not correspond to early morning.

Changed this to "late evening to nighttime"

15. L207: "early morning and early afternoon". Please define this period in the same manner as you have done in other places within the text.

done.

16. Instead of using the temperature as an example in Eq. (7), please use a generic variable, say X, to generalize the RMS difference formula. Moreover, instead of explaining the meaning of i=8 on L220, just mention that the index i denotes a model level.

We think that adding another symbol for "generic variable" is a bit cumbersome at this point in the paper ($\mathbf{x}$ is already representing the entire state vector). The statement about the "top of the PBL" was added at the request of another reviewer. I agree that it is a little too specific. We have changed this as a compromise, but would like to leave in RMS definition using temperature.

17. Statements regarding the corrections made to the WV profile at 22 UTC (L262, L270-L271 and L302-303). The analyzed WV profile overshoots the observed one only with respect to the MYNN simulation. By contrast, the forecasted values in the MYJ WV profiles are already higher, so increasing the WV values following the DA update acts to further increase the observation misfit. Please make sure to make this distinction while describing your results.

We don't quite agree here, though a change is needed. The MYJ WV forecast is high nearer the top of the PBL, but near the surfact it is a bit low. The PBLH assimilation only contains a single piece of information, it can only push the profile in one direction, and here it pushed it higher. Increasing the RMS differences. We have changed the text slightly.

18. Justification regarding the deteriorated estimates of the U profile (L266-L268). The authors correctly acknowledge that the estimation of U is a challenging task when one assimilates integrated quantities like PBLH. However, a similar inference can be made in terms of the Vcomponent profile of the wind and, in fact, further argued that the estimation of V is more challenging due to the presence of sharp gradients in the 750-800 hPa layer (cf. lower-right panels in Figs. 6 and 7). An alternative hypothesis to explain the reported differences in the U and V estimates can be linked to the magnitude of the cross-variable ensemble covariances. The lower two panels of Fig. 8, for example, show that the PBLH-V cross-covariances are much larger than their PBLH-U counterparts. Taking into account that the performance of EnOI (and all other ensemble-based DA methods) is especially susceptible to number of ensemble members, it is quite possible that the small PBLH-U covariances are simply a manifestation of the inherent sampling noise, which would in turn act to degrade the quality of the analyzed U profiles. In theory, the above hypothesis could be tested by comparing results with different ensemble sizes (or with different number of vertical model profiles in the context of this study).

This may be a good explanation as well. We don't think that it can be resolved without the implementation of an EnKF. We have added a little along the lines of your suggestions. This is added after the $\mathbf{P}^f\mathbf{H}^T$ plots are introduced.

19. L272-L276: The description of how the PBLH retrievals correct the state variables should be either removed or relocated to the methodology section.

We have removed these lines.

20. L284-287: Here the authors state that the "... more limited velocity corrections are largely constrained by the correlations ...". This is only partially true as Fig. 8 shows that the V crosscovariances are considerably larger than their U counterparts.

This is a little to simplistic an argument. What matters is the relative size of the covariance between nighttime and late afternoon. The magnitude of the temperature and WV covariance increase by

an order of magnitude, whereas the velocity covariances (while changing sign) don't increase in magnitude nearly as much. We have changed this statement slightly in the text.

21. L311: Replace "covariances" with "ensemble covariances" to emphasize the underlying computational method.

Done.

22. L311: It will be best to change "defined" to "controlled". The ensemble covariances are defined mathematically through the sample covariance formula, but controlled by the characteristics of the T, MV, U and V profiles that enter the PBL parameterization schemes.

Done.

23. L314: Did you intend to refer to the "analysis profiles" instead of the "forecast profiles" here?

This should be forecast, and we have changed it.

Typos and stylistic changes

1. The authors should consider segmenting their results in Section 3 with a view of enhancing the readability of their manuscript. One possibility would be to divide the results into three subsections. The first one could discuss the discrepancies between modelled and retrieved PBLH values, the second one – how the assimilated PBLH observations correct the observed and unobserved model variables, while the third might focus on interpreting the magnitude of the T, MV, U and V corrections at 04 UTC and 22 UTC.

We have divieded this section into 3 subsections as you suggest.

2. The paragraph starting on L255 could be merged with the preceding one as it provides a summary of the main results.

Done.

3. Please correct the spelling of EnKF on L325 and L329.

Done.

4. There were several places where "Doppler" was not capitalized.

This has been corrected.

5. I spotted unintended word repetitions in a couple of places within the text, e.g. L252, L255 and L303.

These have been removed.

6. L23: "leading to an increased differences" – remove "an".

Done.

7. L36: "... rapidly transported within this layer". It is not clear which layer is being referred to as the previous sentence mentions both the CBL and SBL.

changed this to "rapidly transported within the CBL".

8. L38: "The PBLH is fundamental to ...". This sentence provides a very general description on the significance of PBLH and should be mentioned earlier in the paragraph, e.g. after the sentence starting on L32.

This sentence was combined with the first sentence in the introduction.

9. L42: "penetrates the top" could be changed to "penetrates its top" to make it clear that the authors refer to the PBL top.

Done.

10. L186: "This system is solved...". Which system? Please be more specific by listing the relevant equations.

Changed to identify the analysis equations as being solved.

11. L208: "... the MYJ for (red triangles) both are higher than the observations". Please confirm that "both" refers to the MYJ forecasts in the early morning and early afternoon. If this is the case, remove "both" as it is clear from the context. and 8 UTC) ..."] makes it hard to interpret the sentence starting on L225.

We have changed this sentence to indicate both "MYJ"(red triangles) and "MYNN" (blue squares) are be referred to.

13. L232: "increase" should be replaced with "increases".

Instead we changed "difference" to "differences" and "analysis" to "analyses".

14. L237: "(0.5m/2 decrease)" should be replaced with "(0.5m/s decrease)".

Done.

15. L240: "inthe RMS differences" – please separate "in" from "the".

done.

16. L249-L250: "In the late afternoon (Figures 6,7) indicate . . . " – please remove the brackets and refine the sentence structure.

done.

17. L260: "The WV profile is shown to be increased . . . ". It is the WV values that increase, not the profile itself.

Removed "profile".

18. L270: Remove "in" from "in show that".

Done.

19. L279: "We can also analyze this . . . ". Not clear what "this" refers to, please clarify.

Changed "this" to "the assimilation".

20. L321-L322: "will require the construction of an EnkF, and run over many days" – please correct the wording in this sentence.

We have changed this sentence slightly.

Figures

1. It would be useful to label the figure panels with (a), (b), etc.

Done.

2. Please avoid repetitions in the title and axis labels (e.g., potential temperature in the upperleft panel of Fig. 5).

This has been changed to avoid the repetition.

3. Legends are sitting atop some of the curves in Figs. 4-7. Please make sure that all data is displayed in the revisited figures.

We have left in only one legend for each set of 4 plots so that the curves are no longer covered.

4. Fig. 8: Please include the ensemble covariance units on the x-axis. Please also replace "for PBL physics model MYHH" to "for the MYNN PBL scheme".

Done.

References

Anderson, J. L., 2003: A local least squares framework for ensemble filtering. Mon. Wea. Rev., 131, 634–642, https://doi.org/10.1175/1520-0493(2003)131¡0634:ALLSFF¿2.0.CO;2.

Bannister, R. N., H. G. Chipilski, and O. Martinez-Alvarado, 2020: Techniques and challenges in the assimilation of atmospheric water observations for numerical weather prediction towards convective scales. Q. J. R. Meteorol. Soc., 1–48, https://doi.org/10.1002/qj.3652.

Bishop, C. H., 2016: The GIGG-EnKF: Ensemble Kalman filtering for highly skewed nonnegative uncertainty distributions. Q. J. R. Meteorol. Soc., 142, 1395–1412, https://doi.org/10.1002/qj.2742.

Bocquet, M., C. A. Pires, and L. Wu, 2010: Beyond gaussian statistical modeling in geophysical data assimilation. Mon. Wea. Rev., 138, 2997–3023, https://doi.org/10.1175/2010MWR3164.1.

Burgers, G., P. J. Van Leeuwen, and G. Evensen, 1998: Analysis scheme in the ensemble Kalman filter. Mon. Wea. Rev., 126, 1719–1724, https://doi.org/10.1175/1520- 0493(1998)126¡1719:ASITEK¿2.0.CO;2.

Chipilski, H. G., X. Wang, and D. B. Parsons, 2020: Impact of assimilating PECAN profilers on the prediction of bore-driven nocturnal convection: A multiscale forecast evaluation for the 6 July 2015 case study. Mon. Wea. Rev., 148, 1147–1175, https://doi.org/10.1175/MWR-D-19-0171.1.

Cohn, S., 1997: An Introduction to Estimation Theory. J. Meteorol. Soc. Japan, 75, 257–288, https://doi.org/10.1248/cpb.37.3229. Coniglio, M. C., G. S. Romine, D. D. Turner, and R. D. Torn, 2019: Impacts of Targeted AERI and Doppler Lidar Wind Retrievals on Short-Term Forecasts of the Initiation and Early Evolution of Thunderstorms. Mon. Wea. Rev., 147, 1149–1170, https://doi.org/10.1175/MWR-D-18-0351.1.

Dee, D. P., and A. M. da Silva, 2003: The Choice of Variable for Atmospheric Moisture Analysis. Mon. Wea. Rev., 131, 155–171, https://doi.org/10.1175/1520- 0493(2003)131¡0155:TCOVFA¿2.0.CO;2.

Degelia, S. K., X. Wang, and D. J. Stensrud, 2019: An Evaluation of the Impact of Assimilating AERI Retrievals, Kinematic Profilers, Rawinsondes, and Surface Observations on a Forecast of a Nocturnal Convection Initiation Event during the PECAN Field Campaign. Mon. Wea. Rev., 147, 2739–2764, https://doi.org/10.1175/mwr-d-18-0423.1. ——, ——, ——, and D. D. Turner, 2020: Systematic evaluation of the impacts of assimilating a network of ground-based remote sensing profilers for forecasts of nocturnal convection initiation during PECAN. Mon. Wea. Rev., in press, https://doi.org/https://doi.org/10.1175/MWR-D-20-0118.1.

Evensen, G., 1994: Sequential data assimilation with a nonlinear quasi-geostrophic model using Monte Carlo methods to forecast error statistics. J. Geophys. Res., 99, https://doi.org/10.1029/94jc00572.

noindent Evensen, G., 2003: The Ensemble Kalman Filter: Theoretical formulation and practical implementation. Ocean Dyn., 53, 343–367, https://doi.org/10.1007/s10236-003-0036-9.

Fletcher, S. J., and M. Zupanski, 2006: A data assimilation method for log-normally distributed observational errors. Q. J. R. Meteorol. Soc., 132, 2505–2519.

Hu, J. U. N. J. U. N., N. Yussouf, D. D. Turner, T. A. Jones, and X. U. G. U. A. N. G. Wang, 2019: Impact of ground-based remote sensing boundary layer observations on short-term probabilistic forecasts of a tornadic supercell event. Wea. Forecasting, 34, 1453–1476, https://doi.org/10.1175/WAF-D-18-0200.1.

Kamineni, R., T. N. Krishnamurti, R. A. Ferrare, S. Ismail, and E. V. Browell, 2003: Impact of High Resolution Water Vapor Cross-Sectional Data on Hurricane Forecasting. Geophys. Res. Lett., 30, 1234, https://doi.org/10.1029/2002GL016741. 9

NRC, 2009: Observing Weather and Climate from the Ground Up. National Academies Press, 250 pp.

Oke, P. R., J. S. Allen, R. N. Miller, G. D. Egbert, and P. M. Kosro, 2002: Assimilation of surface velocity data into a primitive equation coastal ocean model. J. Geophys. Res. Ocean., 107, 1–25, https://doi.org/10.1029/2000jc000511.

Assimilation of lidar planetary boundary layer height observations.

Andrew Tangborn[1], Belay Demoz[1,2], Brian J. Carroll[2], Joseph Santanello[3]and Jeffrey L. Anderson[4]

[1]Joint Center for Earth Systems Technology, University of Maryland Baltimore County, Baltimore, MD, USA

[2]Dept. of Physics, University of Maryland Baltimore County, Baltimore, MD, USA

[3]Hydrological Sciences Laboratory, NASA Goddard Space Flight Center, Greenbelt, MD, USA

[4]National Center for Atmospheric Research, Boulder, CO, USA

Corresponding author: Andrew Tangborn, tangborn@umbc.edu

Abstract

Lidar backscatter and wind retrievals of the planetary boundary layer height (PBLH) are assimilated into 22 hourly forecasts from the NASA Unified - Weather and Research Forecast (NU-WRF) model during the Plains Elevated Convection Convection at Night (PECAN) campaign on July 11, 2015 in Greensburg, Kansas, using error statistics collected from the model profiles to compute the necessary covariance matrices. Two separate forecast runs using different PBL physics schemes were employed, and comparisons with 6 independent radiosonde profiles were made for each run. Both of the forecast runs accurately predicted the PBLH and the state variable profiles within the planetary boundary layer during the early morning, and the assimilation had a small impact during this time. In the late afternoon, the forecast runs showed decreased accuracy as the convective boundary layer developed. However, assimilation of the ~~doppler~~ Doppler lidar PBLH observations were found to improve the temperature and V velocity profiles relative to independent radiosonde profiles. Water vapor was ~~over corrected~~overcorrected, leading to ~~an~~ increased differences with independent data. Errors in the U velocity were made slightly larger. The computed forecast error covariances between the PBLH and state variables were found to rise in the late afternoon, leading to the larger improvements in the afternoon. This work represents the first effort to assimilate PBLH into forecast states using ensemble methods.

1 Introduction

The planetary boundary layer (PBL) plays an important role in ~~both weather~~and ~~climate .~~ weather, climate and pollution through its role in land-atmosphere interactions and mediation of Earth's water and energy cycles (Santanello et al. 2018). This layer is where the Earth's surface interacts with the atmosphere, exchanging momentum, heat, moisture and pollutants. The PBL height (PBLH) is central to these interactions and is controlled by the energy flux from the surface. Under certain conditions during daytime it defines the convective boundary layer (CBL) and during nighttime it is the stable (non-convective) boundary layer (SBL). Trace gases and aerosols emitted from the surface are rapidly transported within ~~this layer~~ the CBL by turbulent atmospheric motion, and transfer of energy and mass into the free troposphere occurs across an interfacial layer at the top of the PBL. The ~~PBLH is fundamental to weather, climate, atmospheric turbulence and pollution through its role in land-atmosphere interactions and mediation~~

~~of Earth's water and energy cycles (Santanello et al. 2018). It~~ PBL affects convection in the troposphere, which is generally initiated within the boundary layer and then penetrates ~~the~~ its top (Hong and Pan, 1998; Browning, et al. 2007). Thus, accurate knowledge of the PBLH is essential for both weather, pollution and climate forecasting.

The PBLH is defined by thermodynamic properties such as a temperature inversion or hydrolapse which can be measured by radiosonde. Alternatively, the drop off in aerosol concentration that occurs across the top of the PBL is used, since aerosols are well mixed throughout the PBL when the CBL is present (Hicks, et al., 2019). Atmospheric models rely on parameterization schemes to define the structure of the PBL and compute PBLH. These are generally either local mixing schemes that use local turbulent kinetic energy (TKE, Janjic, 1994) or non-local flux schemes (Hong and Pan, 1996). Generally, these PBL parameterizations have systematically higher PBLH relative to observed values (Hegarty et al., 2018), and also have difficulties modeling the growth of the convective layer during the morning. The variety of definitions of PBLH make it difficult to effectively evaluate existing models or develop new ones.

Observations of PBLH are traditionally made by radiosonde measurements, which have high vertical resolution but are expensive to launch frequently and are thus limited to special experiments and/or ill-timed launches (*e.g.* 00/12 UTC National Weather Service launches) with respect to convective and stable PBL development. Likewise, spaceborne measurements of the lower troposphere from passive and active instruments are severely limited in vertical, spatial, and/or temporal resolution (Wulfmeyer et al. 2015). Ground based measurement of PBLH has been proposed for an extensive network of ceilometers by adding to the functionality of instruments that were designed for measuring cloud heights (Hicks et al., 2016). The ceilometer measures the time required for a laser pulse to return to a receiver, from which the height of the scattering is determined. The intensity of the backscatter is correlated with the density of aerosols at a given height and the PBLH is inferred from the location of the maximum negative gradient of the backscatter intensity. Several algorithms employ wavelet transforms to identify the location of the negative gradient (e.g. Brooks, 2003; Knepp, *et al.*, 2017). This existing network of ceilometers could be used to create a relatively dense network of frequent PBLH observations, as was recommended by the 2009 study from the National Research Council (NRC, 2009) and the Thermodynamic Profiling Technologies Workshop (NCAR, 2012).

Since the ceilometer PBLH observations were not yet available for the ~~campaign we are using~~time period we are studying, we employ ~~doppler~~ Doppler lidar observations made at the ~~PECAN~~ Plains Elevated Convection at Night (PECAN) site in Greensburg, Kansas, to demonstrate the methodology. ~~The data~~ PECAN was an intensive campaign to study organized Mesoscale convection systems (MCSs) during the period June 1-July 15, 2015. It employed three aircraft and a large array of ground based lidar, radar and ground weather stations. The data we are using is from a Leosphere WINDCUBE-200S Doppler lidar owned and operated by the University of Maryland, Baltimore County (Delgado et al., 2016). This lidar operates at an infrared wavelength, and hence receives its strongest backscattered signal within the aerosol-laden PBL and is often below the measurement noise floor above the PBL. The Doppler shift of the backscattered signal is used to calculate wind speed as a function of range, which can then be used to produce a multitude of wind and turbulence variables useful for PBL characterization (e.g. vertical velocity variance and signal-to-noise ratio variance). While Doppler lidars and ceilometers are similar in aerosol detection, a Doppler lidar's additional wind measurement capability makes it more broadly applicable and at times more accurate than a ceilometer for PBLH ~~measurement~~retrievals. The PBLH algorithm applied for this study combines several such aerosol and wind variables ~~for PBLH measurement. Each PBLH~~ and each PBLH retrieval involves measurement of turbulence intensity, horizontal wind profiles and backscatter intensity. The heights of steep gradients in these quantities are determined using empirical thresholds and wavelet transform techniques, and the three estimates are combined using fuzzy logic. This is described at length in Bonin et al. (2018). Additional lidar parameters and the application of the algorithm to PECAN data were presented in Carroll et al. (2019). The PBLH ~~measurements~~ retrievals were made from a repeating 25-minute lidar scan cycle. This Doppler lidar and PBLH algorithm combination are generally well-suited for accurate and precise measurement of the PBLH during the daytime boundary layer, nocturnal boundary layer, and morning transition period (Bonin et al. 2018, Carroll et al. 2019). The evening transition is the most challenging for this setup due to due to difficulties in defining a clear mixing layer during the decay of a turbulent daytime PBL (Lothon et al. 2014).

The question remaining is how to assimilate these observations into a numerical weather prediction (NWP) model. A number of studies have explored assimilating ~~thermodynamic~~ boundary layer wind profile measurements from lidar (Hu et al. 2019, Coniglio et al. 2019,

Degelia et al. 2019) and have shown that this increases the accuracy of ~~model PBLH estimates. But we~~ forecasts due to improvements within the PBL. And further studies (Degelia et al. 2020; Chipilski et al. 2020) found that convective initiation (CI) was enhanced through the assimilation of thermodynamic profiles within the PBL, though the former found that CI was degraded by the assimilation of kinematic (velocity) profiles. This work highlights the important role that the PBL plays in forecasting convective events, so that any observations that can improve estimation of the model state should be an important source of new information. We are interested assimilating the PBLH observations directly because the ceilometer network described above will focus on these retrievals, and satellite missions which measure PBLH are also planned. PBLH is a diagnostic variable in NWP parameterized physics models. This means any correction to PBLH will be lost during the model forecast unless the PBLH height observation is used to correct state variables such as temperature and moisture. This could be done either by ~~creating an adjoint of the PBL parameterization~~ adopting a variational data assimilation scheme, or through the use of an ensemble Kalman filter which would determine the error covariances between PBLH and state variables in the model. We choose the latter so as to avoid the task of linearizing the model physics. The structure of the covariance, and how the state variables are changed by assimilating PBLH, will depend on which PBL scheme is used. We will show how such a system could work by conducting a posteriori lidar PBLH observation impact experiments using forecast fields from a NASA Unified - Weather and Research Forecast (NU-WRF, Lidard-Peters, 2015) model runs for one day during the Plains Elevated Convection at Night (PECAN) campaign on July 11, 2015. The assimilation is done on 22 hourly WRF forecast fields throughout the day without cycling the analysis fields back into the model, using two different PBL parameterizations. In this paper, we demonstrate a new and promising method that uses the lidar-based aerosol backscatter and wind derived PBLH to correct model forecasted state variables. The purpose here is to show how ensemble computed error covariance can transfer observational information from PBLH to the state variable profiles.

2 Methodology

The assimilation methodology is based on the ensemble Kalman filter (EnKF)(Evenensen, 1994; Burgers, et al. 1998; Evensen, 2009), where the analysis state is the estimate with ~~the minimum estimated errors~~a minimized error norm, relative to the given error statis-

tics. It differs from the EnKF in that the analysis is not used as an initial state for the next model forecast. Rather, two existing one day NU-WRF forecasts, with different PBL physics schemes, are used when lidar measurements are available at a single location. These forecasts were produced as a part of the PECAN campaign in 2015, and we resuse them here to demonstrate the assimilation algorithm that we have developed. These were not ensemble forecasts so we cannot build a standard ensemble Kalman filter from them. Instead we use Ensemble Optimal Interpolation (EnOI), in which profiles from neighboring model gridpoints are used to obtain an estimate of error statistics (Oke, *et al.*, Evensen, 2003; 2010; Keppenne, *et al.*, 2014). This approach will allow for the construction of the vertical component of covariance, which is needed in order to understand how PBLH can be used to correct atmospheric profiles through the use of profile and PBLH statistics. We use profiles from nearby model grid points and have tested the system with varying numbers of grid points in the ensemble. An ensemble Kalman filter would likely give different covariance information, but the basic relationship between the state variable profiles and the PBLH are determined by the model in the same manner here.

The NU-WRF simulations, taken from existing forecast runs used for the PECAN campaign (Santanello *et al.*, 2019) are initialized using a National Center for Environmental Prediction (NCEP) Global Forecast System (GFS) reanalysis. The two NU-WRF simulations use the Mellor–Yamada–Janjic (MYJ)[Mellor and Yamada, 1974, 1982; Janjic, 2002] and Mellor-Yamada-Nakanishi-Niino level 2.5 (MYNN) [Nakanishi and Niino, 2009] which are local 1.5 and 2.5 order turbulence closure schemes respectively. The PBLH in each of these models is estimated using the ~~total~~ turbulent kinetic energy (TKE) method. The NU-WRF forecast state variables are temperature (T), ~~moisture~~ specific humidity (Q) and velocity (U,V), and we define the forecast vector $\mathbf{x}^f = [T^f \ Q^f \ U^f \ V^f \ (PBLH)^f \ ]$, where we have combined PBLH with the state variables to enable the covariance calculation between them. The vector $\mathbf{x}$ is a column vector, so that the error covariance defined below only includes vertical covariances. The forecast runs are initiated from the NOAA global forecast system (GFS) reanalysis interpolated to the local domain of 30-48N and 84-110 W, with 220×220 lat/lon and 54 vertical levels, at 0 UTC. At this time, the initial state has assimilated all of the convential and satellite observations globally. The two WRF forecast experiments start at 0 UTC, and are run for 22 and 23 hours for the MYJ and MYNN experiments, respectively. We use an ensemble of the 20×20 nearest gridpoints, so that all of the ensemble members are within about 30 km of the lidar obser-

vations (since the grid spacing is about 3 km). Generally, larger ensembles using grid-points farther away will result in larger forecast error covariance because the geographic variability. So this ensemble size was chosen as a balance between ensemble size and geographic localization. The forecast standard deviation for PBLH on the chosen ensemble was around 27 m at 22 UTC. Lidar PBLH observations were made every 25 minutes on that day in Greensburg, KS (37.6 N, 99.3 W), while balloon soundings were launched from that location 6 times as part of the Plains Elevated Convection At Night (PECAN; Gerts et al. 2017).

~~The forecast error covariance, $\mathbf{P}^f$ is defined as~~

$$\mathbf{P}^f = \left\langle (\mathbf{x}^f - \mathbf{x}^t)(\mathbf{x}^f - \mathbf{x}^t)^T \right\rangle$$

~~where the summation is over the grid points $i = 1, N_{lon}$, $j = 1, N_{lat}$ and $\mathbf{x}^t$ is the (unknown) true state, on the discrete model grid. We only assimilate the observation $y^o = PBLH = H(\mathbf{x}^f)$~~ For an EnKF the generalized analysis equations are:

$$\mathbf{x}^a = \mathbf{x}^f + \mathbf{K}(\mathbf{y}^o - H(\mathbf{x}^f)) \tag{1}$$

where $\mathbf{x}^a$ is the analysis state, $\mathbf{x}^f$ is the forecast state, $\mathbf{y}^o$ is the observation vector and H is the non-linear observation operator. The ~~analysis equation is~~

$$\mathbf{x}^a = \mathbf{x}^f + \mathbf{K}(y^o - H(\mathbf{x}^f))$$

~~where the~~ gain matrix, $\mathbf{K}$ is defined by:

$$\mathbf{K} = \mathbf{P}^f\mathbf{H}^T(\mathbf{H}\mathbf{P}^f\mathbf{H}^T + (\sigma^o\mathbf{R})^2)^{-1}, \tag{2}$$

~~σ^o is the observation error~~ and $\mathbf{P}^f$ is the forecast error covariance, $\mathbf{R}$ is the observation error covariance and $\mathbf{H}$ is the linearized observation operator. The matrices $\mathbf{P}^f\mathbf{H}^T$ and $\mathbf{H}\mathbf{P}^f\mathbf{H}^T$ are formed from the ensemble of forecasts. In the present work, we use the EnOI method, and assimilate observations one at a time using the the ensemble of profiles described above. In this case, $\mathbf{x}^a$ and $\mathbf{x}^f$ depend only only vertical level, and $\mathbf{y}^o = y^o$, $\mathbf{R} = (\sigma^o)^2$ and $\mathbf{H}\mathbf{P}^f\mathbf{H}^T = (\sigma^f)^2$ become scaler quantities. The analysis equations are then

.02in

$$\mathbf{x}^a = \mathbf{x}^f + \mathbf{K}(y^o - H(\mathbf{x}^f)) \tag{3}$$

and

$$\mathbf{K} = \mathbf{P}^f\mathbf{H}^T((\sigma^f)^2 + (\sigma^o)^2)^{-1}, \tag{4}$$

The observation error standard deviation supplied ~~with the lidar retrievals, and~~ by the lidar retrieval is σ^o, which is determined from the combined uncertainty of the vertical velocity variance, velocity gradient and backscatter gradient. Generally, when these quantities change rapidly at the top of the PBL, then the estimated error is small. The error estimates are larger when (during the evening), the gradients are much more gradual. $\mathbf{H}$ is the linearized observation operator for PBLH. Because the PBLH is related to the state variables via the two PBL physics schemes, determining $\mathbf{H}$ would require linearizing the PBL physics at every analysis time. Rather, here we use the EnOI described above to get:

$$\mathbf{P}^f\mathbf{H}^T \approx \left\langle (\mathbf{x}^f - {\mu_\mathbf{x}}^f)\ (H(\mathbf{x}^f - {\mu_\mathbf{x}}^f))^T \right\rangle \tag{5}$$

and

$$\mathbf{H}\mathbf{P}^f\mathbf{H}^T = (\sigma^f)^2 \approx \left\langle H(\mathbf{x}^f - {\mu_\mathbf{x}}^f)\ (H(\mathbf{x}^f - {\mu_\mathbf{x}}^f))^T \right\rangle \tag{6}$$

where ${\mu_\mathbf{x}}^f$ is the mean forecast state of the ensemble of profiles. See Houtekamer and Zhang (2016) for a review of ensemble Kalman filter techniques.

We expect the correlation between the airmass within the PBL and the free troposphere to drop away rapidly, because of limited intereactions between them. We found that this can cause errors in the analysis profiles if error covariance between the state variables and PBLH is allowed to continue into the troposphere. To reduce these errors we have added an exponential decay starting at the model level closest to the PBLH (k_{PBLH}) to define a vertical localization factor:

$$C_{loc} = exp\left[-\alpha(\frac{k - k_{PBLH}}{k_{PBLH}})^2\right] \tag{7}$$

where k is the model level and $\alpha = 8$ is an experimentally determined factor. ~~This ensures~~ The factor C_{loc} is multiplied by the vertical covariance in (??) to ensure that the covariance between the PBLH and the state variables becomes small within a couple of model levels into the free troposphere.

~~This system is~~ Equations ??-?? are solved at each hour using the nearest lidar profile observation in time, and the resulting analysis fields are compared to radiosonde profiles when the latter are also available. There are 22 or 23 analyses (for each forecast run), and 6 times where comparison with radiosonde profiles are made. We focus on the impact of the assimilation on the state variables T, Q, U and V rather than the PBLH because only the state variables would be retained by a forecast.

3 Results

~~The~~ This section describes the NU-WRF ~~simulations, taken from existing forecast runs used for the PECAN campaign (Santanello et al., 2019) are initialized using a National Center for Environmental Prediction (NCEP) Global Forecast System (GFS) reanalysis. The two forecast runs were conducted using MYJ PBL physics (2-22 UTC) and MYNN (2-23 UTC) on July 11, 2015. Lidar PBLH observations were made every 25 minutes on that day in Greensburg, KS (37.6 N, 99.3 W), while balloon soundings were launched from that location 6 times as part of the Plains Elevated Convection At Night (PECAN; Gerts et al. 2017).~~ simulation results, the assimilation of PBLH into these forecasts, and the relationship between the assimilation impact and the time varying forecast and observation error covariances.

3.1 NU-WRF simulations

The one day NU-WRF simulations are presented in this section. Figure **??** shows the PBLH during that day, derived from the two NU-WRF forecasts, lidar observations and soundings. We have determined the sounding PBLH using the parcel method (Holzworth, 1964), which defines the top as the height where the potential temperature first exceeds the ground temperature. The lidar PBLH (black *, derived using the method reported in Bonin, 2018) closely matches the radiosonde estimates (green triangles) in the late evening to ~~early morning~~ nighttime (2-7 UTC), while it is somewhat lower ~~in the afternoon~~ late afternoon to early evening (18-24 UTC). The two NU-WRF forecasts differ from the observations depending on the time of day. ~~In the early morning and early afternoon the MYJ forecasts~~ During nighttime and early morning the MYJ (red triangles) ~~both~~ and MYNN (blue squares) forecasts are higher than the observations, then rise less than the lidar observations in the late morning and early afternoon (12-17 UTC, there are no radiosonde measurements to compare to here) before rising much higher than the observations in the late afternoon (18-24 UTC).

3.2 Impact of assimilation on state variables

Since we are primarily interested in the impact of the assimilation on state variables within the boundary layer, in Figures **??** and **??** we plot the RMS difference between the model and the independent (unassimilated) radiosonde profiles from the sur-

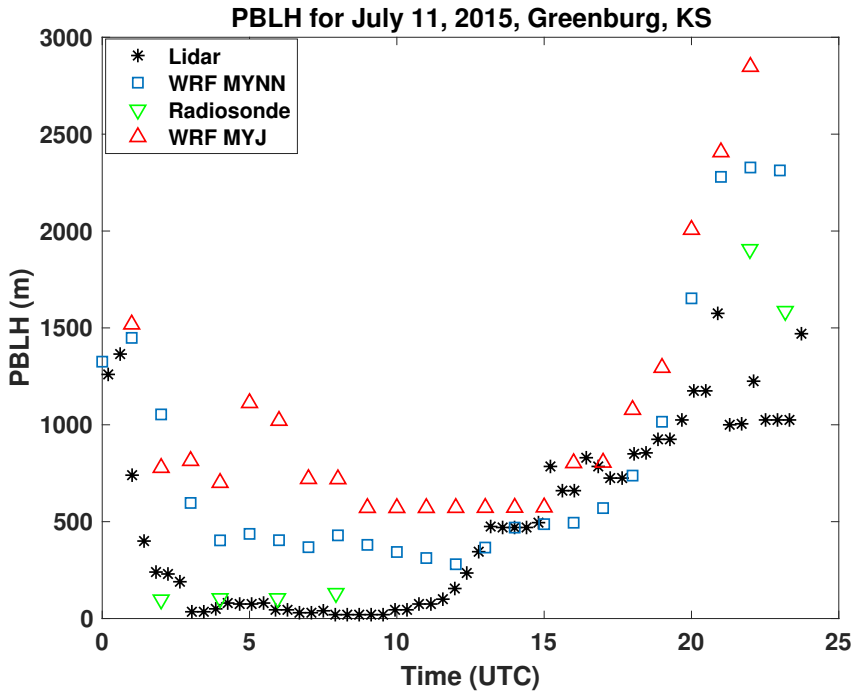

c

Figure 1. PBLH vs UTC time for July 11, 2015 for lidar backscatter (black *), WRF model - MYJ (red triangles), WRF model - MYNN (blue squares), and radiosonde observations using parcel method (green triangles).

face to roughly the top of the boundary layer in the late afternoon. This corresponds to the first 8 layers, or about 800 mb. We use a fixed number of layers so as to make the comparisons of the RMS differences consistent during the day, rather than computing the RMS over a different number of layers as the PBL grows during the day. For the temperature forecast, the RMS difference would is

.05in

$$RMS(t_a) = \left[\frac{1}{8}\sum_{i=1}^{8}(T_i^f - T_i^{sonde})^2\right]^{1/2} \quad (8)$$

.05in where t_a is the analysis time and ~~$i = 8$ is~~ "i" represents the model level~~at the top of the PBL in the late afternoon~~. Figures **??** and **??** show the RMS differences with the radiosonde profiles throughout the day for the forecasts (blue x) and analyses (red squares) for potential temperature (~~upper left~~a), water vapor mixing ratio WV (~~upper right~~b) and the U (~~lower left~~c) and V (~~lower right~~d) components of velocity.

During the night (2-9 UTC), the assimilation has a relatively smaller impact on the potential temperature RMS differences (upper left) in the early morning (6 and 8 UTC), and the two forecasts have similar accuracy. By late afternoon (22 and 23 UTC, note that the MYJ forecast stops at 22 UTC) the radiosonde comparisons show that the assimilation reduces RMS differences in the potential temperatures by around $1.5K$ for MYJ and $2K$ for MYNN. The water vapor mixing ratio (upper right) also has little impact from the assimilation between 2 and 8 UTC, but at 22 UTC (the next radiosonde profile) the RMS ~~difference~~ differences for both MYJ and MYNN ~~analysis~~ analyses increase by at least $1.5\times10^{-3}kg/kg$ in the late afternoon. The U-velocity profiles (lower right) show small differences between the MYJ and MYNN through 8 UTC (3 a.m. local time) and the assimilation increases the RMS differences with radiosonde profiles by nearly ~~$1m/2$~~ $1m/s$ starting at 22 UTC for both models. The V-velocity profiles (d) begin to differ between MYJ and MYNN for the forecasts at 8 UTC (~~$0.5m/2$~~ $0.5m/s$ decrease), and assimilation also decreases the RMS differences with radiosondes in late afternoon by $1.5 - 2m/s$.

We would like to understand why there is a smaller impact during night time and early morning, whereas there are decreases ~~inthe~~ in the RMS differences in temperature and V velocity and increases in moisture and U velocity in the late afternoon. To this

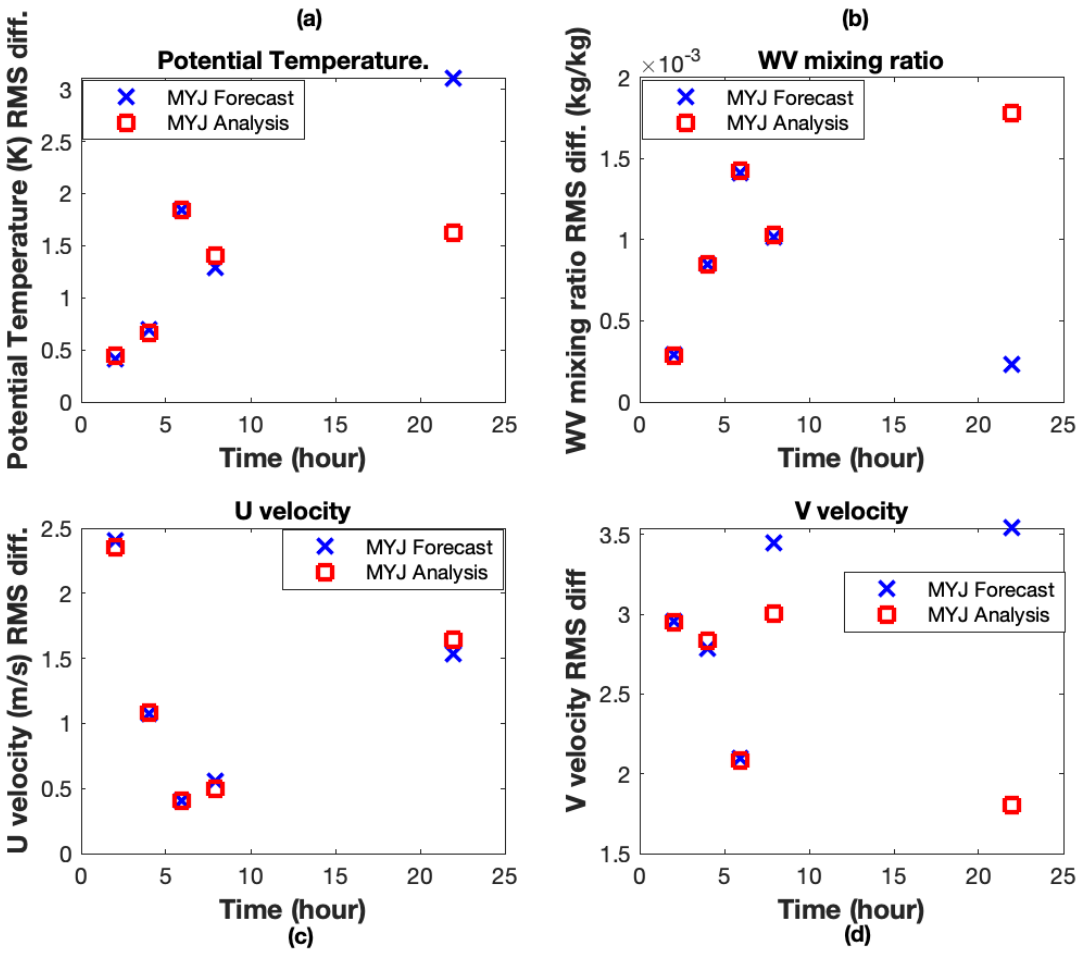

Figure 2. RMS difference for lowest 8 layers, vs. time of forecast (blue x) and analysis (red square) with radiosonde profiles for potential temperature (~~upper left~~a), water vapor (~~upper right~~b), U velocity (~~lower left~~c) and V velocity (~~lower right~~d).

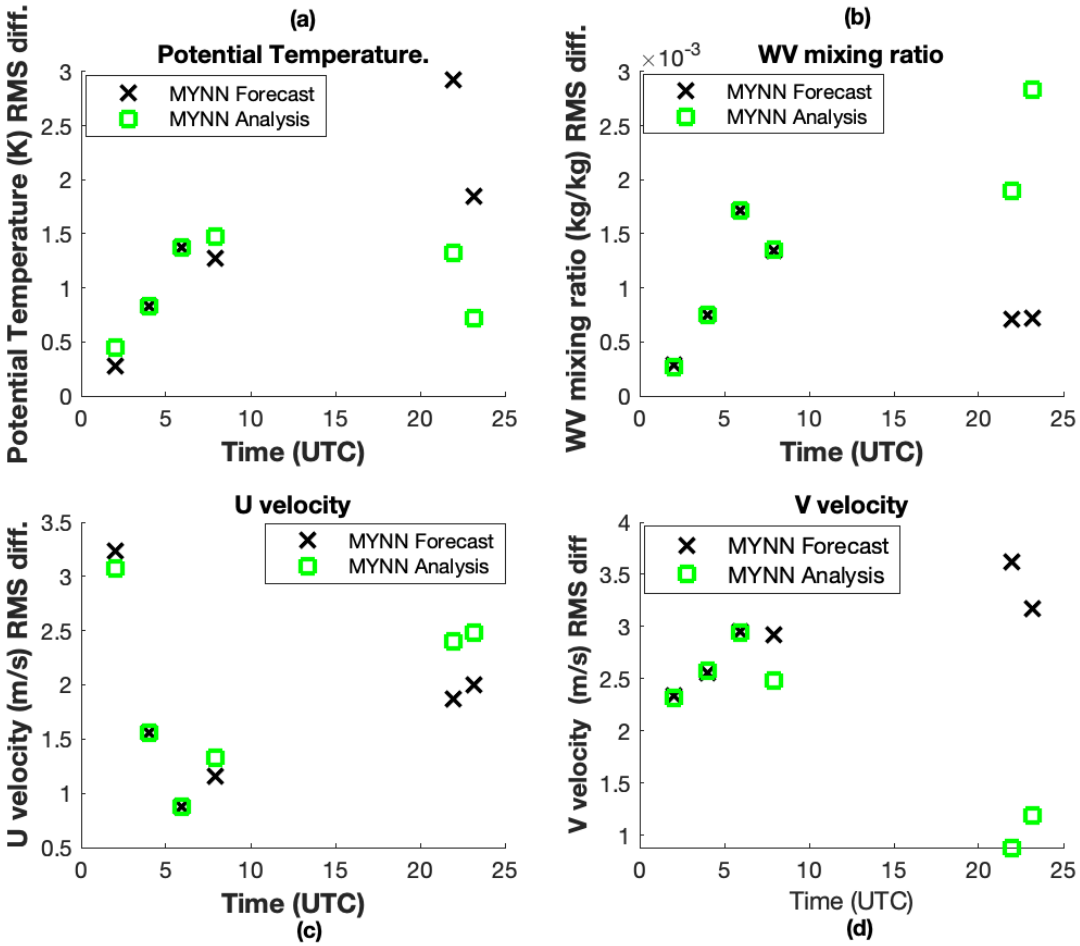

Figure 3. Same as Figure **??**, but for MYNN PBL model, with forecast (black x) and analysis (blue square).

end, we plot the forecast, analysis and radiosonde profiles (T, Q, U and V) at 4 UTC (11 p.m. local time) and 22 UTC (5 p.m. local time) in Figures **??**-**??**. At 4 UTC, (Figures **??**,**??**) these clearly indicate that there are small corrections made by the assimilation, as the red and blue profiles closely overlap. But it also shows that the profiles (particularly temperature and moisture) more accurately follow the radiosonde profiles (except for the U velocity above the PBL), meaning that ~~there is less room for improvement to the forecast state~~that any substantial corrections would have made the profiles worse relative the the radiosonde profiles and ultimately degrade the next PBLH forecast. In contrast, Figure (**??**) shows that the forecast PBLH (~~particulary~~ particularly MYJ) is quite a bit higher than the lidar observation at 4 UTC. In the late afternoon ~~(Figures ?? , ??)~~ Figures **??** and **??** indicate that there are large differences between the ~~forecast~~ forecasts and radiosonde profiles for all of the state variables~~, and the~~ . The forecast PBLH values differ substantially from the lidar measurements as well. The correction to ~~to~~ the forecast profiles generally pushes the analyses towards the independent radiosonde profiles, particularly for temperature and V velocity.

So the forecasts that ~~that~~ predicted both PBLH and state variables with relatively greater accuracy in the early morning were not corrected, while the less accurate afternoon forecast was drawn towards the independent radiosonde measurements. The assimilation also made changes to the vertical velocity (W) in the afternoon, but there is no independent data to compare with so we have not included it.

The WV ~~profile~~ is shown to be increased by the assimilation (since WV and PBLH are negatively correlated and higher PBLH corresponds to lower WV levels in the PBL models), but the analysis overshoots the radiosonde WV profile for MYNN, hence causing the increase in the water vapor RMS difference in Figures **??** and **??**. The MYJ forecast for WV is mostly too high, so the analysis also increases the RMS difference. Compared to temperature, WV is highly variable in time and space and it has been shown in the past that slanted balloon trajectories ~~under estimate~~ underestimate the WV present (Demoz et al 2006; Crook, 1996). The U velocity difference with the radiosonde is larger for the analysis, but this correction is more difficult because the differences (at least for MYJ) are both positive and negative and the PBLH observation only contains a single piece of information. The V velocity is, on the other hand, greatly improved by the assimilation. These analysis profiles ~~in~~ show that, for this one analysis time, the assimilation is pushing the state variables in the proper direction for temperature, V velocity and mois-

ture, though the moisture correction overshoots the readiosonde profile. ~~The reason for these corrections to the state variable profiles is that~~ PBLH is not a prognostic variable, so that the analysis PBLH values are not retained and therefore cannot directly affect the next forecast. But it is important to note that the temperature and moisture profiles are changed by the assimilation in a way that indicates that the next forecast is likely to have a more accurate PBLH estimate. Figures **??** and **??** both show that the level at which the potential temperature begins to rise and the ~~error covariance between PBLH and each state variable, $\mathbf{P}^f\mathbf{H}^T$, can be computed from the ensemble of profiles that was collected from the model grid. The forecast PBLH for each profile was computed using the full PBL physics, and therefore contains the essential correlation information between these variables~~WV mixing ratio begins to drop has been moved to a level much closer to that observed by the lidar. We do not make forecasts from the analysis fields, but these profiles show promise for improved PBLH forecasts when cycling experiments are done in a future implementation.

3.3 Ensemble error covariances

The increasing differences between PBLH and profile forecasts from early morning to late afternoon only partly explain the much larger impact of the assimilation at 22 UTC. We can also analyze ~~this by plotting~~ the assimilation by investigating the error covariance between PBLH and each of the state variables ~~, seen in Figure ?? at different times during the day~~($\mathbf{P}^f\mathbf{H}^T$) and the relative error variances in observation space ($\mathbf{H}\mathbf{P}^f\mathbf{H}^T$ and $\mathbf{R}$). We show $\mathbf{P}^f\mathbf{H}^T$ in Figure **??** for the MYNN PBL physics model at the 6 radiosonde times. The covariance with temperature is always positive, and grows by a factor of 4 by late afternoon near the surface. The covariance with WV is mostly negative and grows by roughly a factor of 5, while the covariance with the two components of velocity oscillate between positive and negative and shows less consistent growth. Thus, the largest impact of assimilation on temperature and moisture occurs in late afternoon while more limited velocity corrections are largely constrained by the correlations determined by the ensemble of model forecast states. In addition, the covariance between PBLH and the U velocity are substantially smaller than those with the V velocity. This means that spurious correlations between PBLH and U might be present, given the relatively small ensemble and the geographic variation of the ensemble members. The error variances are also plotted

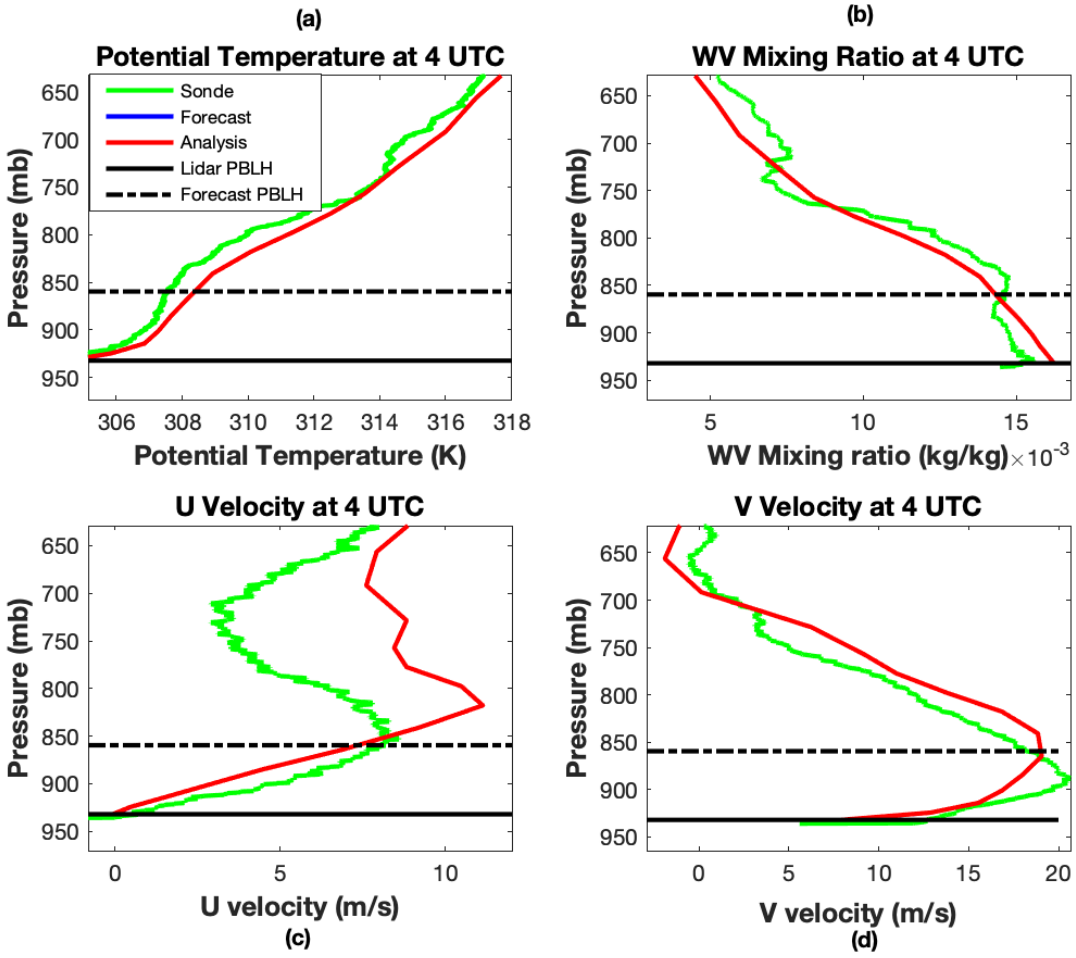

Figure 4. Profiles from radiosonde (green), forecast (blue) and analysis (red) for potential temperature (~~upper left~~a), water vapor mixing ratio (~~upper right~~b), u-velocity (~~lower left~~c) and v-velocity (~~lower right~~d) at 4 UTC, July 11, 2015 in Greensburg, KS. The model uses the MYJ physics parameterization.

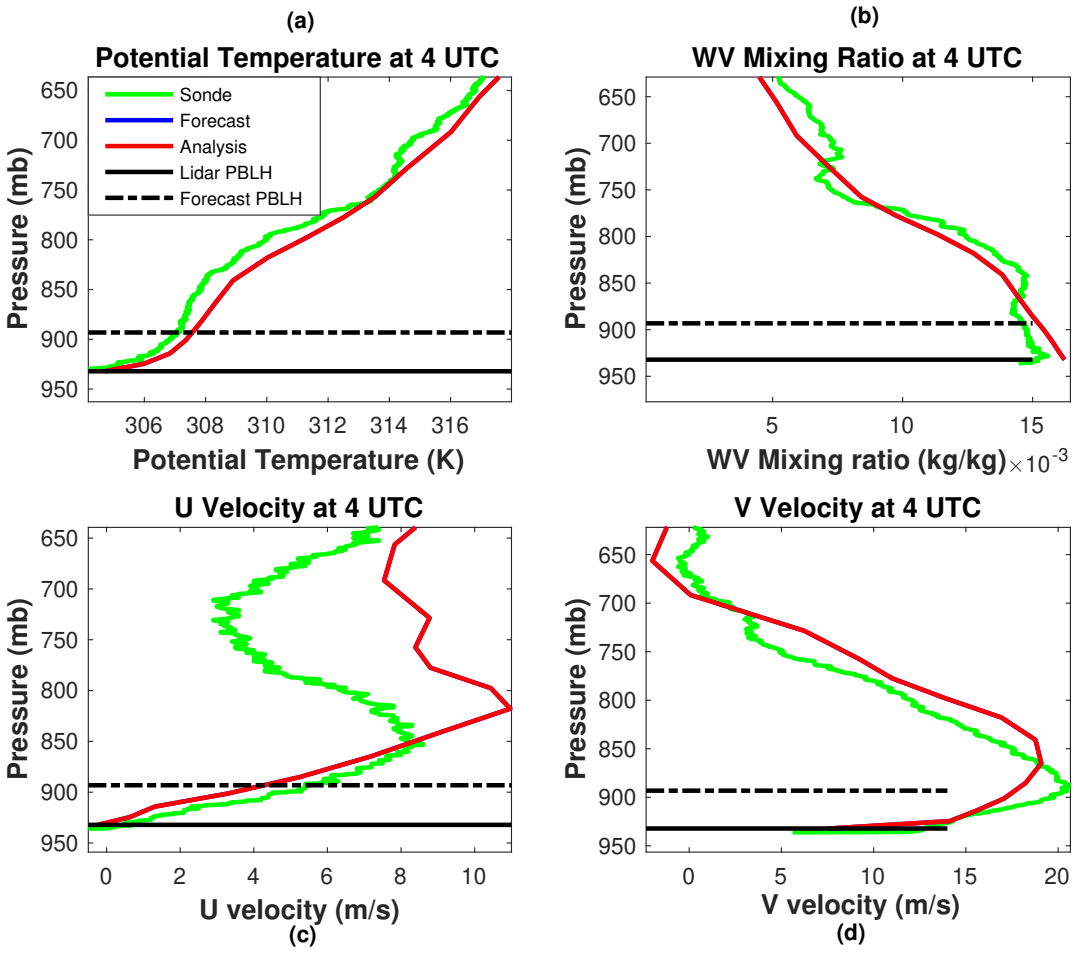

Figure 5. Same as figure **??** except using MYNN model.

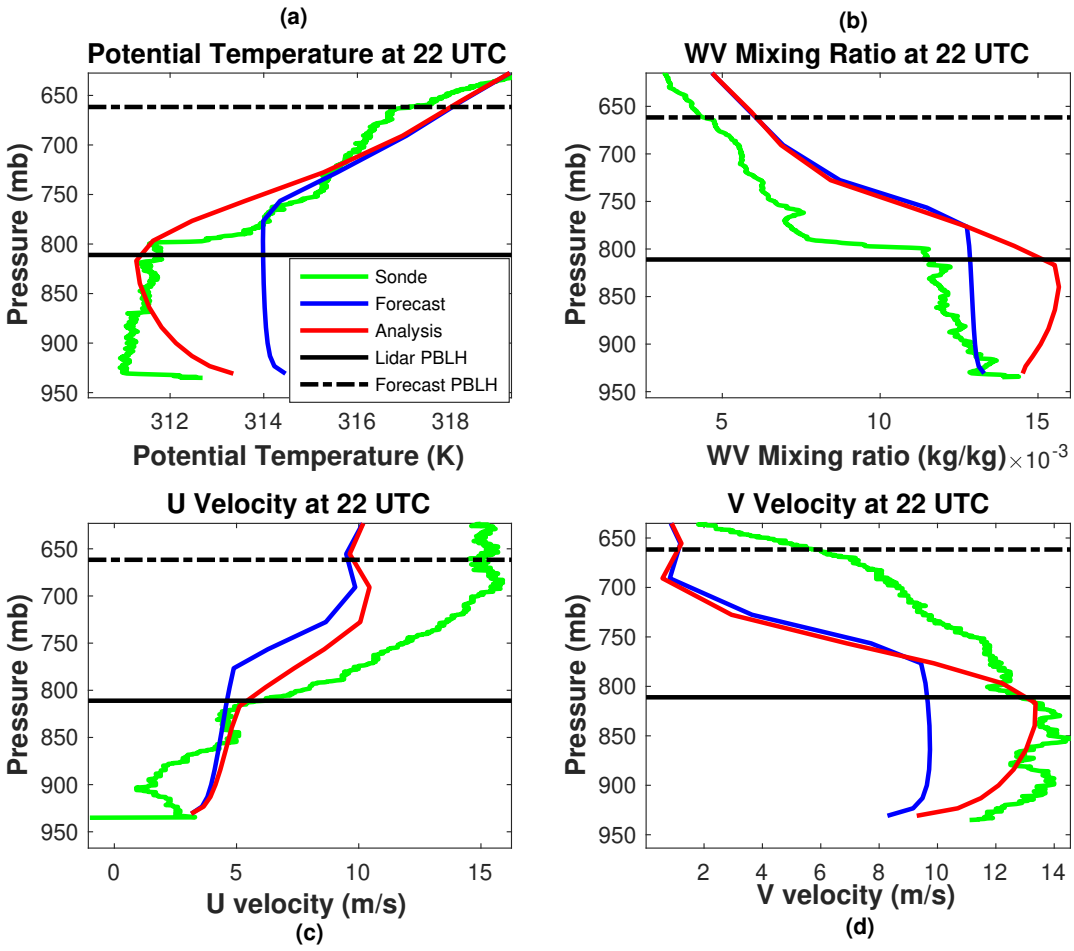

Figure 6. Same as figure **??** except using except at time 22 UTC.

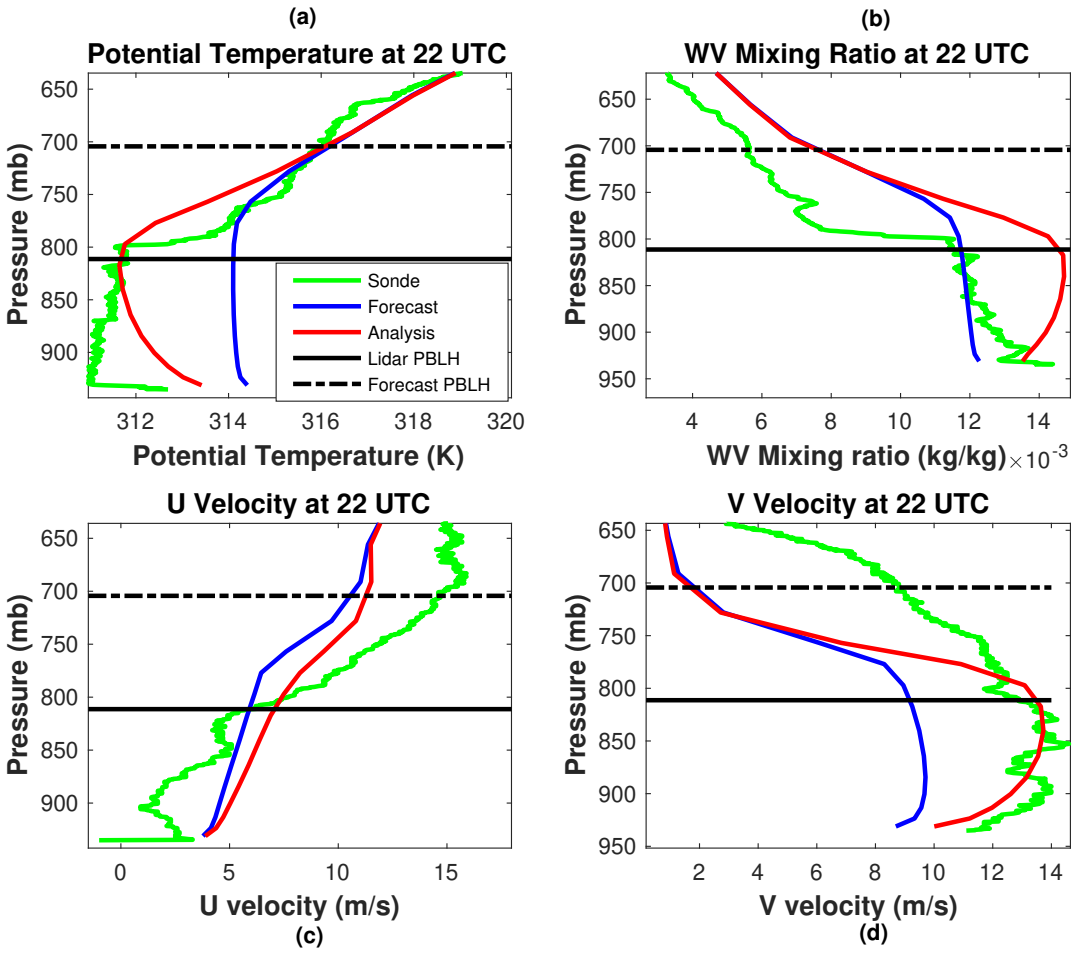

Figure 7. Same as figure **??** except using MYNN model.

346 at the radiosonde times in Figure ??, which shows that the observation errors are much
347 larger than the forecast errors during evening and early morning times (2,4,6,8 UTC)
348 and then become relatively smaller in the late afternoon (22,23 UTC). This is an additional
349 contributing factor to the minimal impact of PBLH observations early in the day and
350 the much larger impact in the afternoon.

(a)

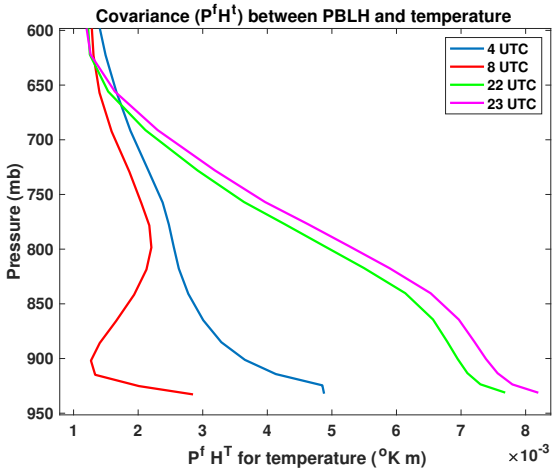

(b)

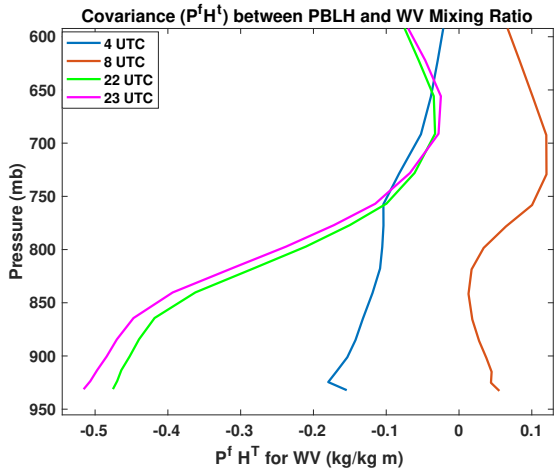

(c)

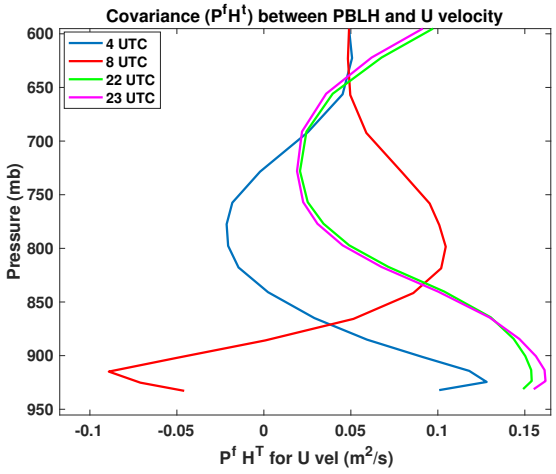

(d)

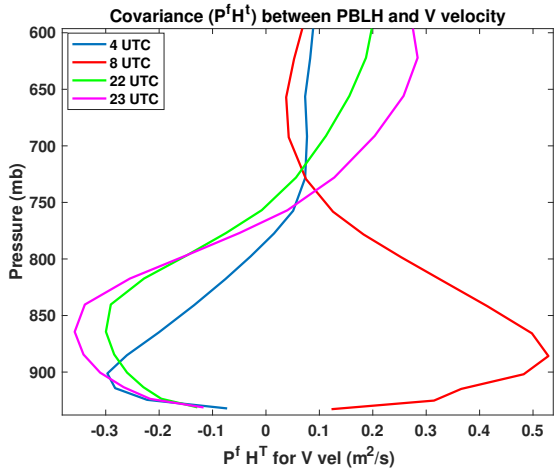

Figure 8. Covariance $\mathbf{P}^f\mathbf{H}^T$ between PBLH and temperature (~~upper left~~a), water vapor (~~upper right~~b), U velocity (~~lower left~~c) and V velocity (~~lower right~~d), at times 4, 8, 22 and 23 UTC, for PBL physics model MYHH.

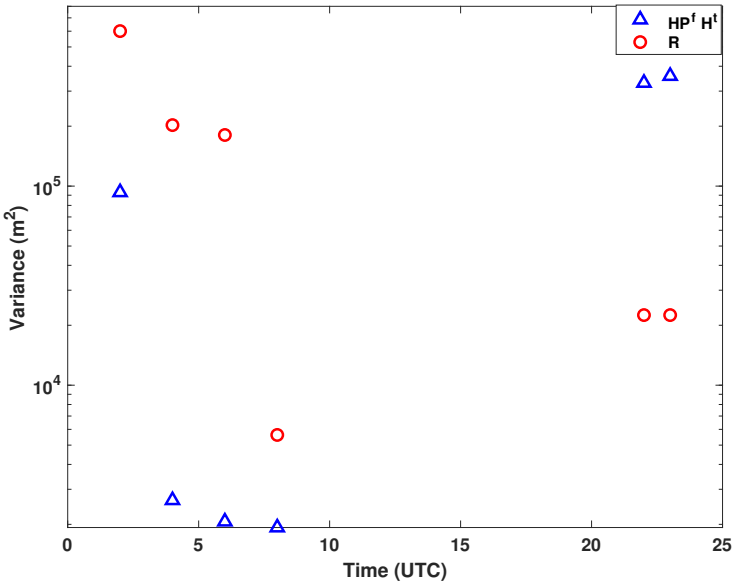

Figure 9. Forecast ($\mathbf{HP}^f\mathbf{H}^t$) and observation ($\mathbf{R}$) error covariance for the PBL physics model MYHH at the 6 radiosonde times.

4 Discussion and Conclusions

These offline data assimilation experiments indicate that assimilating ground based lidar backscatter and wind measurements of PBLH into a regional NWP model will likely lead to corrections to profiles within the PBL, ~~particulary when~~particularly when, in the future, this approach is applied to an EnKF assimilation system with cycling. Using two NU-WRF forecasts over a period of one day with different PBL physics models, we show how the state variables, T, WV, U and V can be corrected using an assimilation system with ensemble based error covariances. During the night and early morning the assimilation has relatively little impact on the state variables, but by late afternoon the temperature field is drawn closer to independent radiosonde measurements. We have shown that the lack of data impact early in the day is the due to the relatively higher accuracy of the model and lack of correlation between the forecast PBLH and temperature profiles at that time. Later in the day, when the model is less accurate in predicting the growth of the boundary layer, the data begins to draw the analyses mostly toward the independent radiosonde profiles. The assimilation ~~over corrected~~ overcorrected the water vapor mixing ratio in the direction of radiosonde data, and this could likely be tuned in an assimilation system. And it corrected the the V velocity component by a smaller amount,

and reduced differences with the radiosonde profiles for the V velocity. These corrections are the result of ensemble computed error covariances between the PBLH and the state variable profiles within the PBL. The results here indicate that this approach has some potential to be used in a forecast system in a way that that the PBLH observational information could be carried forward in time so as to impact the forecast accuracy within the PBL. An additional value of assimilating PBLH is its close connection with the PBL scheme used in the model. The ensemble covariances between PBLH and the different state variables are ~~defined~~ controlled through the PBL physics scheme. This has an impact on the corrections made to the profiles within the PBL, which can be used as another way to evaluate the physics parameterizations. For example, the MYJ and MYNN result in ~~analysis~~ forecast profiles that differ, particularly in WV in the late afternoon. And the differences in reponse to assimilation are an indication of how the two different PBL schemes affect the covariance between PBLH and the state variables. However, a full evaluation would require that the assimilation be implemented into a cycling data assimilation system.

This work is intended only to demonstrate a necessary first step in terms of how ensemble statistics can help to constrain profiles within the PBL by assimilating PBLH observations. A more complete demonstration of this approach will require the construction of an EnKF, ~~and~~ which should be run over many days with a variety of weather patterns, including significantly warmer(cooler) and wetter(drier) days. This is needed to show how the assimilated PBLH observations will impact future forecasts within the PBL. More of the PBL physics schemes need to be investigated as well, since the correlation between PBLH and state variables will vary widely depending on which scheme is used. An estimate of the forward operator error should be included in the algorithm as well. There are also differences in the way PBLH is computed in the PBL physics schemes, and the methods used for radiosonde observations (see Hegarty, et al., 2018). This will impact the manner in which the assimilation and resulting forecasts are validated. The larger uncertainty in the lidar PBLH retrievals during nighttime (Figure **??**) mean that the assimilation will not significantly constrain the model state within the PBL during this period. So it would be very helpful to complement PBLH observations with thermodynamic and kinematic profile observations, partuculary overnight. The fact that PBLH is a non-negative variable means that the O-F statistics will likely be non-Gaussion so that the assimilation

algorithm would need to include an extension to handle this possibility (e.g. Cohn, 1997).

In addition, ~~an EnKf~~ a cycling EnKF will involve spatial covariances in both horizontal and vertical directions, and will allow for both inflation and horizontal localization. This will enable further tuning of the system to optimize the analysis state relative to the independent radiosonde observations. The PBLH assimilation withn the EnKF framework could be done in any of numerous existing ~~enKF~~ EnKF assimilation systems that connect with WRF, including ~~NU-WRf~~ NU-WRF (Lidard-Peters *et al.*, 2015) and WRF-DART (Anderson *et al.*, 2009). Future development of PBLH assimilation algorithms will also need to address the effect of the different definitions of PBLH, such as the TKE method used the physics schemes and the backscatter and wind profile method used in the retrievals.

5 Acknowledgments

A. Tangborn was funded through the JCET cooperative agreement with NASA Goddard Space Flight Center. B. Demoz was funded by National Science Foundation award (AGS-1503563) to the University of Maryland, Baltimore County and through NOAA Cooperative Science Center in Atmospheric Sciences and Meteorology, funded by the Educational Partnership Program at NOAA in collaboration with Howard University. J. Santanello was funded through a NASA Decadal Survey Study Team grant.

The careful reading and comments by Rohith Muraleedharan Thundathil and the three anonymous reviewers has helped to greatly improve the quality of this paper.

6 Data Sets

PECAN (`https://data.eol.ucar.edu/master_list/?project=PECAN\verb`) data are archived by NCAR/EOL, which is funded by NSF. The forecast and analysis fields produced for this work are stored at https://alg.umbc.edu/pecan/.

7 Competing Interests

The authors declare that they have no conflict of interest.

8 Author Contributions

Andrew Tangborn built the assimilation system, with input from Jeffrey Anderson on the algorithm. Belay Demoz and Brian Carroll provided the lidar observations. Joseph Santanello provided background information on PBL physics. All of the authors contributed to writing and revising the paper.

9 References

Anderson, J.L., T. Hoar, K. Raeder, H. Liu, N. Collins, R. Torn and A. Arellano (2009), The Data Assimilation Research Testbed: A Community Facility, *Bull. Amer. Met. Soc.*, 90, 1283-1296 doi:10.1175/2009BAMS2618.1.

Bonin, T.A., B.J. Carroll, R.M. Hardesty, W.A. Brewer, K. Hajney, O.E. Salmon and P.B. Shepson (2018), Doppler Lidar Observations of the Mixing Height in Indianapolis Using an Automated Composite Fuzzy Logic Approach, *J. Atmos. Ocean Tech.*, 35, 473-490.

Brooks, I.M. (2003), Finding Boundary Layer Top: Application of a Wavelet Covariance Transform to Lidar Backscatter Profiles, *J. Atmos. Ocean Tech.*, 20, 1092-1105.

Browning, K. A., and Coauthors (2007), The Convective Storm Initiation Project. , *Bull. Amer. Meteor. Soc.*, 88, 1939–1955, https://doi.org/10.1175/BAMS-88-12-1939.

Burgers, G., P. J. Van Leeuwen, and G. Evensen, 1998: Analysis scheme in the ensemble Kalman filter. Mon. Wea. Rev., 126, 1719–1724, https://doi.org/10.1175/1520- 0493(1998)126¡1719:ASITEK¿2.0.CO;

.1in Carroll, B. J., Demoz, B. B., and Delgado, R. (2019). An overview of low-level jet winds and corresponding mixed layer depths during PECAN. Journal of Geophysical Research: Atmospheres, 124(16), 9141-9160. https://doi.org/10.1029/2019JD030658.

Chipilski, H. G., X. Wang, and D. B. Parsons, 2020: Impact of assimilating PECAN profilers on the prediction of bore-driven nocturnal convection: A multiscale forecast evaluation for the 6 July 2015 case study. Mon. Wea. Rev., 148, 1147–1175, https://doi.org/10.1175/MWR-D-19-0171.1.

.1in Cohn, S., 1997: An Introduction to Estimation Theory. J. Meteorol. Soc. Japan, 75, 257–288, https://doi.org/10.1248/cpb.37.3229.

.1in Coniglio, M. C., G. S. Romine, D. D. Turner, and R. D. Torn, 2019: Impacts of Targeted AERI and Doppler Lidar Wind Retrievals on Short-Term Forecasts of the Initiation and Early Evolution of Thunderstorms. Mon. Wea. Rev., 147, 1149–1170, https://doi.org/10.1175/MWR-D

.1in Coniglio, M. C., G. S. Romine, D. D. Turner, and R. D. Torn, 2019: Impacts of Targeted AERI and Doppler Lidar Wind Retrievals on Short-Term Forecasts of the Initiation and Early Evolution of Thunderstorms. *Mon. Wea. Rev.*, 147, 1149–1170.

Crook, N. A., 1996: Sensitivity of moist convection forced by boundary layer processes to low-level thermodynamic fields. Mon. Wea. Rev., 124, 1767–1785.

Degelia, S. K., X. Wang, and D. J. Stensrud, 2019: An Evaluation of the Impact of Assimilating AERI Retrievals, Kinematic Profilers, Rawinsondes, and Surface Observations on a Forecast of a Nocturnal Convection Initiation Event during the PECAN Field Campaign. *Mon. Wea. Rev.*, 147, 2739–2764.

Degelia, S.K., X. Wang, D.J. Stensrud and D. D. Turner, 2020: Systematic evaluation of the impacts of assimilating a network of ground-based remote sensing profilers for forecasts of nocturnal convection initiation during PECAN. Mon. Wea. Rev., in press, https://doi.org/https://doi.org/10.1175/

.1in Delgado, R., Carroll, B. and Demoz, B. (2016). FP2 UMBC Doppler Lidar Line of Sight Wind Data. Version 1.1 [Data set]. UCAR/NCAR - Earth Observing Laboratory. Accessed 29 May 2017. https://doi.org/10.5065/d6q81b4h.

Demoz, B., C. Flamant, T. Weckwerth, D. Whiteman, K. Evans, F. Fabry, P. Di Girolamo, D. Miller, B. Geerts, W. Brown, G. Schwemmer, B. Gentry, W. Feltz, and Z. Wang, 2006: The dryline on 22 May 2002 during IHOP-2002: Convective scale measurements at the profiling site. Mon. Wea. Rev., 134(1), 294-310.

.1in Evensen, G., 1994: Sequential data assimilation with a nonlinear quasi-geostrophic model using Monte Carlo methods to forecast error statistics. J. Geophys. Res., 99, https://doi.org/10.1029/94jc0057

.1in Evensen, G., 2003: The Ensemble Kalman Filter: Theoretical formulation and practical implementation. Ocean Dyn., 53, 343–367, https://doi.org/10.1007/s10236-003-0036-9.

Evensen, G. (2009), *Data assimilation: the ensemble Kalman filter*, Springer.

Geerts, B., and Coauthors, (2017), The 2015 Plains Elevated Convection At Night field project. *Bull. Amer. Meteor. Soc.*, 98, 767–786, https://doi.org/10.1175/BAMS-D-15-00257.1.

Hegarty, J.D., J. Lewis, E.L. McGrath-Spangler, J. Henderson, A.J. Scarino, P. DeCola, R. Ferrare, M. Hicks, R.D. Adams-Selin and E.J. Welton (2018) Analysis of the Planetary Boundary Layer Height during DISCOVER-AQ Baltimore–Washington, D.C., with Lidar and High-Resolution WRF Modeling, *J. Appl. Meteo. Climat.*, 57, 2679-2696.

Hicks, M., D. Atkinson, B. Demoz, K. Vermeesch and R. Delgado (2016), The National Weather Service Ceilometer Planetary Boundary Layer Project, *The 27th International Laser Radar Conference (ILRC 27)*, https://doi.org/10.1051/epjconf/201611915004.

Hicks, M., B. Demoz, K. Vermeesch and D. Atkinson (2019), Intercomparison of Mixing Layer Heights from the National Weather Service Ceilometer Test Sites and Collocated Radiosondes, *J. Atmos. Ocean Tech.*, 36, 129-137.

Holzworth, G.C. (1964), Estimates of mean maximum mixing depths in the contiguous United States, *Mon. Wea. Rev.*, 92, 235-242.

Hong, S.-Y. and H.-L. Pan (1996), Nonlocal boundary layer vertical diffusion in a medium-range forecast model, *Mon. Wea. Rev.*, 124, 2332-2339.

Hong, S.-Y. and H.-L. Pan (1998), Convective Trigger Function for a Mass-Flux Cumulus Parameterization Scheme, *Mon. Wea. Rev*, 126, 2599-2620.

Houtekamer, P.L. and F. Zhang (2016), Review of the Ensemble Kalman Filter for Atmospheric Data Assimilation, *Mon. Wea. Rev.*, 144, 4489-4532.

Hu, J., N. Yussouf, D. D. Turner, T. A. Jones, and X. Wang, 2019: Impact of Ground-Based Remote Sensing Boundary Layer Observations on Short-Term Probabilistic Forecasts of a Tornadic Supercell Event, *Wea. Forecasting*, 34, 1453–1476.

Janjic, Z.I. (1994), The Step-mountain eta coordinate model: Further developments of the convection, viscous sublayer, and turbulence closure, *Mon. Wea. Rev.*, 122, 927-945.

Janjic, Z.I. (2002), Nonsingular Implementation of the Mellor-Yamada Level 2.5 Scheme in the NCEP Meso model (NCEP Office Note No. 437).

T. N. Knepp, J.J. Szykman, R. Long, R. M. Duvall, J. Krug, M. Beaver, K. Cavender, K. Kronmiller, M. Wheeler, R. Delgado, R. Hoff, T. Berkoff, E. Olson, R. Clark, D. Wolfe, D. Van Gilst, D. Neil (2017), Assessment of mixed-layer height estimation from single-wavelength ceilometer profiles, *Atmos. Meas. Tech.*, 10, 3963-3983.

Lothon, M., Lohou, F., Pino, D., Couvreux, F., Pardyjak, E. R., Reuder, J., et al. (2014). The BLLAST field experiment: Boundary-Layer late afternoon and sunset turbulence. Atmospheric Chemistry and Physics, 14(20), 10931–10960. https://doi.org/10.5194/acp-14-10931-2014.

Mellor, G.L. and T. Yamada (1974), A Hierarchy of Turbulence Closure Models for Planetary Boundary Layers, *J. Atmos. Sci.*, 31, 1791-1806.

Mellor, G.L. and T. Yamada (1982), Development of a turbulence closure model for geophysical fluid problems, *Rev. Geophys.*, 20, 851-875.

Nakashini, M. and H. Niino (2009), Development of an improved turbulence closure model for the atmospheric boundary layer, *J. Met. Soc. Japan*, 87, 895-912.

National Research Council (2009), Observing Weather and Climate from the Ground Up: A Nationwide Network of Networks, in: Observing Weather and Climate from the Ground Up: A Nationwide Network of Networks, 1–234, Natl. Academies Press, 2101 Constitution Ave, Washington, DC 20418 USA.

NCAR Technical Note (2012), Thermodynamic Profiling Technologies Workshop Report to the National Science Foundation and the National Weather Service, National Center for Atmospheric Research.

Oke, P.R., G.B. Brassington, D.A. Griffin, and A. Schiller (2010), Ocean data assimilation: a case for ensemble optimal interpolation, *Austr. Meteor.Ocean. J.*, 59, 67-76.

Peters-Lidard, C.A. and Co-authors (2015), Integrated modeling of aerosol, cloud, precipitation and land processes at satellite-resolved scales, *Environ. Mod. Soft.*, 67, 149-159.

Santanello, J.A. and Co-authors (2018), Land–Atmosphere Interactions: The LoCo Perspective, *Bull. Amer. Meteor. Soc*, https://doi.org/10.1175/BAMS-D-17-0001.1.

Santanello, J.A.,, S.Q. Zhang, D.D. Turner, P. Lawston, and W.G. Blumberg, PBL Thermodynamic Profile Assimilation and Impacts on Land-Atmosphere Coupling, AGU Fall Meeting, San Francisco, CA, Dec. 9-13, 2019.

Wulfmeyer, V., R.M. Hardesty, D.D. Turner, A. Behrendt, M.P. Cadeddu, P. Di Girolamo, P. Schlussel, J.Van Baelen and F. Zus (2015), A review of the remote sensing of lower tropospheric thermodynamic profiles and its indispensable role for the understanding and the simulation of water and energy cycles, *Rev. Geophys.*, https://doi.org/10.1002/2014RG000476.